The Astrophysical Journal Supplement Series, 221:10 (11pp), 2015 November doi:10.1088/0067-0049/221/1/10

FORMALDEHYDE MASERS: EXCLUSIVE TRACERS OF HIGH-MASS STAR FORMATION

E. D. Araya [1], L. Olmi [2,3], J. Morales Ortiz[4], J. E. Brown[1,9], P. Hofner[5,6], S. Kurtz[7], H. Linz[8], and M. J. Creech-Eakman[5]
[1] Western Illinois University, Physics Department, 1 University Circle, Macomb, IL 61455, USA
[2] INAF, Osservatorio Astrofisico di Arcetri, Largo E. Fermi 5, I-50125 Firenze, Italy
[3] University of Puerto Rico, Río Piedras Campus, Physics Department, Box 23343, UPR Station, San Juan, PR 00931, USA
[4] University of Puerto Rico, Río Piedras Campus, Physical Sciences Department, P.O. Box 23323, San Juan, PR 00931, USA
[5] New Mexico Institute of Mining and Technology, Physics Department, 801 Leroy Place, Socorro, NM 87801, USA
[6] National Radio Astronomy Observatory, P.O. Box 0, Socorro, NM 87801, USA
[7] Instituto de Radioastronomía y Astrofísica, Universidad Nacional Autónoma de México, Apdo. Postal 3-72, 58089 Morelia, Michoacán, Mexico
[8] Max-Planck-Institut für Astronomie, Königstuhl 17, D-69117 Heidelberg, Germany
Received 2015 August 10; accepted 2015 September 29; published 2015 October 28

ABSTRACT

The detection of four formaldehyde (H_2CO) maser regions toward young high-mass stellar objects in the last decade, in addition to the three previously known regions, calls for an investigation of whether H_2CO masers are an exclusive tracer of young high-mass stellar objects. We report the first survey specifically focused on the search for 6 cm H_2CO masers toward non high-mass star-forming regions (non HMSFRs). The observations were conducted with the 305 m Arecibo Telescope toward 25 low-mass star-forming regions, 15 planetary nebulae and post-AGB stars, and 31 late-type stars. We detected no H_2CO emission in our sample of non HMSFRs. To check for the association between high-mass star formation and H_2CO masers, we also conducted a survey toward 22 high-mass star-forming regions from a Hi-GAL (*Herschel* infrared Galactic Plane Survey) sample known to harbor 6.7 GHz CH_3OH masers. We detected a new 6 cm H_2CO emission line in G32.74−0.07. This work provides further evidence that supports an exclusive association between H_2CO masers and young regions of high-mass star formation. Furthermore, we detected H_2CO absorption toward all Hi-GAL sources, and toward 24 low-mass star-forming regions. We also conducted a simultaneous survey for OH (4660, 4750, 4765 MHz), H110α (4874 MHz), HCOOH (4916 MHz), CH_3OH (5005 MHz), and CH_2NH (5289 MHz) toward 68 of the sources in our sample of non HMSFRs. With the exception of the detection of a 4765 MHz OH line toward a pre-planetary nebula (IRAS 04395+3601), we detected no other spectral line to an upper limit of 15 mJy for most sources.

Key words: ISM: molecules – masers – radio lines: ISM

1. INTRODUCTION

The 6 cm line of formaldehyde (H_2CO) has been intriguing since its discovery. Soon after the first detection toward the Galactic center (Snyder et al. 1969), Palmer et al. (1969) found H_2CO absorption in cold dust clouds that have no background radio continuum other than the cosmic microwave background. A non-thermal mechanism was necessary to explain such a detection, i.e., a mechanism that "refrigerates" the transition to an excitation temperature below 2.73 K. Based on quantum mechanical calculations, Garrison et al. (1975; see also Townes & Cheung 1969) demonstrated that H_2–H_2CO collisions at densities below 10^6 cm^{-3} were responsible for the supercooling of the 6 cm H_2CO line.

In 1974, Downes & Wilson detected 6 cm H_2CO emission blended with absorption toward the high-mass star-forming region NGC 7538; the emission was later shown to be a maser (Forster et al. 1980; Rots et al. 1981). The detection of widespread H_2CO absorption (which indicated large quantities of H_2CO in the interstellar medium), and the detection of maser emission in NGC 7538, motivated a series of surveys for H_2CO masers in the 1980s (e.g., Forster et al. 1985). Surprisingly, new H_2CO masers were detected only toward one other region in the Galaxy (Srg B2; Whiteoak & Gardner 1983).

The detection of H_2CO maser emission toward NGC 7538 IRS1 and later toward Sgr B2 (two prominent sites of high-mass star formation), guided subsequent surveys to be conducted toward high-mass star-forming regions (e.g., Mehringer et al. 1995), resulting in the detection of an H_2CO maser in G29.96−0.02 (Pratap et al. 1994). Motivated by the apparent association of H_2CO masers with very young high-mass stellar objects, we conducted three surveys toward high-mass star-forming regions and detected four new H_2CO maser sites (Araya et al. 2004, 2007b, 2008).

A large number of non-high-mass star-forming regions (non HMSFRs) have been observed in the 6 cm H_2CO transition (mainly for absorption studies; e.g., Dieter 1973; Heiles 1973; Minn & Greenberg 1973; Sandqvist & Lindroos 1976; Martin & Barrett 1978; Goss et al. 1980; Sandqvist & Bernes 1980; Vanden Bout et al. 1983; Pettersson 1987; Zhou et al. 1990; Turner 1994; Moore & Marscher 1995; Young et al. 2004; Araya et al. 2006b)[9], and none has revealed clear signs of emission in this transition. Thus, it seems that H_2CO masers are indeed a phenomenon exclusively associated with high-mass star formation. However, a targeted search designed to detect H_2CO masers toward non HMSFRs has not been conducted until now.

The need for a targeted survey comes from the weak intensity of the known H_2CO masers (typically $\sim$ 100 mJy). Such weak emission can be easily masked by the ubiquitous and strong 6 cm H_2CO absorption. Thus, observations conducted with relatively small telescopes (and consequently large beamwidths) such as the H_2CO survey by Dieter (1973),

[9] Currently at Department of Physics and Astronomy, University of Missouri Columbia.

[9] Other studies, blind surveys among them, have included non HMSFRs in the samples: e.g., Whiteoak & Gardner (1974), Few (1979), Downes et al. (1980), Rodríguez et al. (2006).

Table 1
Observed Transitions Toward the Sample of Non HMSFRs

Molecule	Rest Frequency (MHz)	Reference
OH	4660.2420	Pickett et al. (1998)[a]
OH	4750.6560	Pickett et al. (1998)[a]
OH	4765.5620	Pickett et al. (1998)[a]
H_2CO	4829.6594[b]	Tucker et al. (1970)
H110α	4874.1570[c]	Gordon & Sorochenko (2002)
HCOOH	4916.3120	Lovas, F. J.[d]
CH_3OH	5005.3208	Müller et al. (2004)
CH_2NH	5289.8130	Lovas, F. J.[d]

Notes.
[a] See Harvey-Smith & Cohen (2005) for an energy level diagram.
[b] Weighted average rest frequency of the $F = 2$–2 and $F = 0$–1 components.
[c] The central bandpass rest frequency was set to 4875.3500 MHz to include the He110α and C110α lines.
[d] NIST Recommended Rest Frequencies by F. J. Lovas (http://physics.nistgov/PhysRefData/Micro/Html/contents.html); see also Pickett et al. (1998).

are not well suited to detect H_2CO masers. Indeed, as exemplified by GBT observations of G29.96−0.02 (Sewiło et al. 2004), H_2CO masers can be masked by H_2CO absorption even at the angular resolution of a 100 m telescope (half power beam width HPBW $\sim 2'.5$).

Observations of the 6 cm H_2CO line toward non HMSFRs at high angular resolution ($\lesssim 60''$) have been reported toward a relatively small number of sources. Specifically, $\lesssim 60''$ resolution observations have been reported toward only a handful of late-type stars (Forster et al. 1985; Araya et al. 2003), regions of low-mass star formation (including prestellar cores; Colgan et al. 1986; Zhou et al. 1990; Kalenskii et al. 2004; Young et al. 2004; Araya et al. 2006b), and diffuse molecular clouds (Marscher et al. 1993; Araya et al. 2014), all resulting in no detection of H_2CO emission.

In this work we present the first survey dedicated to the search for 6 cm H_2CO masers toward non HMSFRs, specifically toward late-type stellar objects and regions of low-mass star formation. Our goal is to assess whether 6 cm H_2CO masers are an exclusive phenomenon of high-mass star formation, thus we also conducted a survey toward a sample of high-mass star-forming regions.

2. OBSERVATIONS

2.1. Low-mass Star-forming Regions and Evolved Stars

Because 6 cm H_2CO masers are weak and may be easily masked by extended H_2CO absorption, a telescope with high sensitivity and small beamwidth is required for the survey, and

Table 2
Observed Sources I: Low-mass Star-forming Regions

Source	α(2000) (h m s)	δ(2000) (° ′ ″)	H_2O Masers	Source Type
L1448-IRS2	03 25 22.4	+30 45 11	N	Class 0
L1448-IRS3	03 25 36.3	+30 45 15	N	Class 0
IRAS 03245+3002	03 27 39.0	+30 12 59	Y	Class 0/I
IRAS 03258+3104	03 28 55.4	+31 14 35	Y	Class 0
HH12	03 29 03.6	+31 16 04	Y	Class 0
NGC1333-IRAS4A	03 29 10.5	+31 13 32	Y	Class 0
IRAS 03282+3035	03 31 20.4	+30 45 25	N	Class 0
B1-IRS	03 33 15.9	+31 07 34	Y	Class 0
HH211-FIR	03 43 57.1	+32 00 50	N	Class 0
B5-IRS	03 47 41.6	+32 51 47	N	Class I
IRAS 04016+2610	04 04 43.5	+26 18 58	N	Class I
IRAS 04108+2803	04 13 53.6	+28 11 23	N	Class I
IRAS 04113+2758	04 14 26.5	+28 06 01	N	Class I
IRAS 04158+2805	04 18 58.0	+28 12 24	N	Class I
IRAS 04166+2706	04 19 42.7	+27 13 40	N	Class 0/I
IRAS 04169+2702	04 19 58.6	+27 10 04	N	Class I
T Tau South	04 21 59.2	+19 32 06	Y	Class II
IRAS 04239+2436	04 26 56.9	+24 43 36	N	Class I
L1527	04 39 53.9	+26 03 10	N	Class 0/I
IRAS Z04489+3032[a]	04 52 09.4	+30 37 48	N	Class II[b]
FU-Ori[c]	05 45 22.4	+09 04 12	N	Class I/II[d]
S68N	18 29 48.1	+01 16 51[e]	Y	Class 0
L723-FIR	19 17 53.9	+19 12 20	Y	Class 0
B335-IRS	19 37 00.8	+07 34 11	N	Class 0
IRAS 20050+2720MMS1	20 07 06.8	+27 28 59	Y	Class 0/I

Notes. Sample selected from the Furuya et al. (2003) H_2O survey. H_2O maser detection and source type are as reported by Furuya et al. (2003).
[a] This source is listed in Furuya et al. (2003) as IRAS 04489+3032 and L1513 (see also Bontemps et al. 1996), and corresponds to the YSO Haro 6-39 according to Simbad.
[b] Protostellar class from Andrews & Williams (2005); listed as Class I in Furuya et al. (2003).
[c] Incorrect coordinates listed in Furuya et al. (2003); the correct coordinates were used in this work.
[d] Based on the SED, this source is in a transition between Class I and II (see, e.g., Quanz et al. 2007; Green et al. 2013), though it has been listed as Class I by Gramajo et al. (2014).
[e] There is a typo in the declination of this source as listed in Table 1 of Furuya et al. (2003); the correct coordinates were used in this work.

Table 3
Observed Sources II: Oxygen-rich Late Type Stars

Source	α(2000) (h m s)	δ(2000) (° ′ ″)	H_2O Masers	SiO Masers	OH Masers	Spectral Type
R Com	12 04 15.2	+18 46 57	Y	Y	Y	M5e-M8ep
RT Vir	13 02 38.0	+05 11 08	Y	Y	Y	M8III
RX Boo	14 24 11.9	+25 42 15	Y	Y	N	M6.5e-M8IIIe
S Crb	15 21 24.0	+31 22 03	Y	Y	Y	M6e-M8e
S Ser	15 21 39.5	+14 18 53	Y	Y	Y	M5e-M6e
WX Ser	15 27 47.0	+19 33 52	Y	Y	Y	M8e
IRC+00266	15 28 43.7	+03 49 43	Y	N	Y	M8
U Her	16 25 47.5	+18 53 33	Y	Y	Y	M6.5e-M9.5e
V2108 Oph	17 14 19.0	+08 55 59	Y	Y	Y	M7-M9.8
RT Oph	17 56 32.0	+11 10 10	Y	Y	Y	M7e(c)
V1111 Oph	18 37 19.3	+10 25 42	Y	Y	Y	M4III-M9
X Oph	18 38 21.1	+08 50 03	Y	Y	Y	M5e-M9e
IRC+10374	18 43 33.9	+13 57 31	Y	Y	Y	M8III
V1366 Aql	18 58 30.0	+06 43 02	Y	Y	Y	…
R Aql	19 06 22.4	+08 13 48	Y	Y	Y	M5e-M9e
V1368 Aql	19 09 08.4	+08 16 34	Y	Y	Y	…
OH65.4+1.3	19 51 21.5	+29 12 59	Y	Y	Y	…
SY Aql	20 07 05.8	+12 57 07	Y	Y	Y	M5e-M7e
UX Cyg	20 55 05.5	+30 24 52	Y	Y	Y	M4e-M6.5e
IRAS 21120+0736	21 14 29.6	+07 48 35	Y	…	Y	…
IRAS 21174+1747	21 19 45.0	+18 00 26	Y	…	Y	…
IRAS 22402+1045	22 42 46.8	+11 00 51	Y	…	Y	…
R Peg	23 06 38.9	+10 32 38	Y	Y	Y	M6e-M9e

Note. Sample selected from the Benson et al. (1990) survey. Information about detection of H_2O, SiO, and OH masers, and Spectral Type classification is from Benson et al. (1990).

Table 4
Observed Sources III: Carbon Stars

Source	α(2000) (h m s)	δ(2000) (° ′ ″)
CGCS1779	07 35 46.8	+09 35 59
CGCS1741	07 32 05.7	+15 25 19
CGCS1810	07 39 39.3	+12 02 39
CGCS1953	07 56 53.9	+09 42 46
CGCS2150	08 20 06.0	+02 45 52
CGCS2156	08 20 41.4	+05 11 22
CGCS6306	08 45 22.4	+03 27 12
CGCS2301	08 41 50.0	+07 26 19

Note. Sample selected from Alksnis et al. (2001).

Table 5
Observed Sources IV: Post-AGB, Pre-planetary Nebulae, and Planetary Nebulae

Source	α(2000) (h m s)	δ(2000) (° ′ ″)	Source Type
IC 351	03 47 32.9	+35 02 49	PN
IC 2003	03 56 22.0	+33 52 31	PN
IRAS 04296+3429	04 32 57.0	+34 36 13	post-AGB/PPN
K 3-66	04 36 37.2	+33 39 30	PN
IRAS 04395+3601	04 42 53.6	+36 06 54	post-AGB/PPN
IRAS 05089+0459	05 11 36.2	+05 03 26	PPN?
IRAS 05113+1347	05 14 07.8	+13 50 28	post-AGB/PPN
IRAS 05341+0852	05 36 55.0	+08 54 08	post-AGB/PPN
IRAS 05381+1012	05 40 57.1	+10 14 25	post-AGB/PPN
M 1-5	05 46 50.0	+24 22 03	PN
K 3-70	05 58 45.3	+25 18 43	PN
K 4-48	06 39 55.9	+11 06 30	PN
HD 51585	06 58 30.3	+16 19 25	PPN?
IRAS 07134+1005	07 16 10.3	+09 59 49	PPN?
IRAS 07430+1115	07 45 49.8	+11 08 25	PPN?

Note. Sample from Kohoutek (2001). For some sources (IRAS 04296+3429, IRAS 04395+3601, IRAS 05113+1347, IRAS 05341+0852, IRAS 05381+1012) the coordinates listed here are slightly different than those reported in Kohoutek (2001). In these cases, the coordinates are within ∼1″ from Simbad coordinates (Zacharias et al. 2003).

thus we used the 305 m Arecibo Telescope.[10] The Arecibo Telescope is the most sensitive instrument available for spectral line observations at $\lambda \sim 6$ cm and the single-dish telescope of smallest beamwidth (∼1′). The observations were conducted on 2008 February 1–3, and May 10. We used the C-Band receiver that allows observations in dual linear polarization mode. On February 1, R Com, RT Vir, and RX Boo were observed with the interim spectrometer (two spectral windows to simultaneously observe the H_2CO and H110α lines). The setup of the H_2CO spectral window was: bandwidth BW = 6.25 MHz (∼400 km s^{-1}), 2048 channels, $\Delta\nu$ = 3.05 kHz (0.19 km s^{-1}); the setup of the H110α spectral window was: BW = 12.5 MHz (∼770 km s^{-1}), 2048 channels, $\Delta\nu$ = 6.10 kHz (0.38 km s^{-1}). In the other runs we used the WAPP backend with a bandwidth of 6.25 MHz (∼400 km s^{-1}), 2048 channels, channel separation of 3.05 kHz (0.19 km s^{-1}), and 9 level sampling. The WAPP backend enables simultaneous observations of eight different lines, thus, in addition to

[10] The Arecibo Observatory is operated by SRI International under a cooperative agreement with the National Science Foundation (AST-1100968), and in alliance with Ana G. Méndez-Universidad Metropolitana, and the Universities Space Research Association.

Table 6
Observed Sources V: High-mass Star-forming Regions

Source	α(2000) (h m s)	δ(2000) (° ′ ″)	S_{ν,CH_3OH} (Jy)	$S_{\nu,OH}$ (Jy)
G32.11+0.09	18 49 37.7	−00 41 00	1.2	⋯
G32.74−0.07	18 51 21.8	−00 12 05	48	0.56
G33.13−0.09	18 52 07.9	+00 08 13	11	0.04
G33.61−0.03	18 52 49.0	+00 35 46	0.07	⋯
G34.37+0.23	18 53 13.6	+01 23 31	1.6	⋯
G34.08+0.01	18 53 30.5	+01 02 03	0.73	⋯
G34.71−0.59	18 56 48.2	+01 18 46	0.01	0.02
G35.13−0.74	18 58 06.0	+01 37 06	32	3.92
G35.14−0.75	18 58 09.9	+01 37 27	1.7	⋯
G36.42−0.16	18 58 23.2	+03 02 11	0.03	⋯
G37.04−0.03	18 59 04.2	+03 38 34	9.6	0.05
G37.19−0.41	19 00 43.4	+03 36 24	0.07	⋯
G37.86−0.60	19 02 36.0	+04 07 03	0.19	⋯
G38.93−0.36	19 03 42.0	+05 10 23	0.04	⋯
G39.99−0.64	19 06 39.9	+05 59 13	0.02	⋯
G43.10+0.04	19 09 59.7	+09 03 58	0.02	⋯
G43.53+0.01	19 10 52.9	+09 25 44	0.09	⋯
G45.87−0.37	19 16 42.9	+11 19 10	0.02	⋯
G46.32−0.25	19 17 09.0	+11 46 24	0.02	⋯
G56.96−0.23	19 38 16.8	+21 08 07	1.1	⋯
G59.78+0.63	19 41 03.0	+24 01 15	0.03	⋯
G59.63−0.19	19 43 49.9	+23 28 37	0.58	0.01

Note. Positions and peak flux densities of 6.7 GHz CH_3OH and 6.035 GHz OH masers are from Olmi et al. (2014). The typical rms of the 6.035 GHz OH non-detection from Olmi et al. (2014) was between ∼5 and 10 mJy.

H_2CO, we observed transitions of OH, CH_3OH, HCOOH, CH_2NH, and the H110α line. Table 1 lists the rest frequencies of the observed transitions.

We used position switching mode in all observations, with a typical integration time of 5 minutes ON-source, except for the sample of carbon stars that were observed only 1 minute ON-source. The OFF-source (reference) positions were selected such that the telescope followed the same azimuth/zenith angle track as during the ON-source observations. A calibration signal (noise diode) was observed during 10 s at the end of every scan for antenna temperature calibration.

In this survey we focus on low-mass star-forming regions, late-type stars including oxygen-rich late type, carbon, post-AGB stars, pre-planetary nebulae (PPN) and planetary nebulae (PN). We observed 71 sources: 25 low-mass star-forming regions, 31 late-type stars (23 oxygen-rich late type stars and 8 carbon stars), and 15 post-AGB stars/PPN/PN. Since the known H_2CO masers arise from rich maser environments (e.g., Hoffman et al. 2003), we selected low-mass star-forming regions and oxygen-rich late type stars known to harbor other types of masers. The low-mass star-forming regions are from the catalog of Furuya et al. (2003); we selected all H_2O maser sources observable with the Arecibo Telescope and complemented the sample with non-H_2O maser regions also from Furuya et al. (2003). Most of these sources have been classified as Class 0 and/or Class I, which means that they harbor a protostar that is accreting material and which is bright in the mid-infrared or at least the far-infrared wavelength range. The oxygen-rich late type stars were selected from Benson et al. (1990); carbon stars were selected from Alksnis et al. (2001); PN and post-AGB sources are from Kohoutek (2001).

We present the observed sample in Tables 2–5. The data reduction and calibration were done in IDL[11] using standard Arecibo data reduction routines. The ON and OFF-source scans were separately inspected to check for radio interference and emission/absorption at the reference position.

We conducted "spider" scans (two sets of orthogonal cross scans, each pair rotated by 45° with respect to the other) toward four quasars (B1218+339, 3C286, B2338+132, and B2353+154) to check the telescope pointing and gain, and to measure the telescope beamwidth. The pointing accuracy was better than 10″ and as good as ∼2.″5; the telescope gain varied between 6.2 (at low elevation) and 8.7 K Jy^{-1} (at higher elevation). We measured a HPBW of ∼0.′95. Based on the 3C286 observations (which is a standard VLA flux density calibrator) we estimate that the absolute flux density calibration is better than 30%.

We also observed two sources for system checking: IRAS18566+0408 and B2338+132. The measured flux density of B2338+132 is 344 mJy, which is within 2% of the expected value of 339 mJy (value obtained using the Arecibo IDL routine `fluxsrc`). An estimate of the calibration error can also be obtained from the H_2CO absorption in IRAS 18566+0408, which is extended and thus expected to be constant (Araya et al. 2004). We find that the integrated flux density of the H_2CO absorption in IRAS 18566+0408 differs by less than 4% with respect to the Arecibo observations of Araya et al. (2004). We found no evidence for polarized emission/absorption, and thus after flux density calibration, the two orthogonal polarization spectra were averaged. With the exception of sources affected by H_2CO absorption in the reference position (see below), we fitted and removed linear baseline functions.

In the case of nine low-mass star-forming regions, we detected H_2CO absorption toward the OFF-source position. We calibrated these sources as follows. (1) We obtained the flux density calibrated (ON–OFF)/OFF spectra, i.e., the difference between the ON-source and OFF-source spectra, divided by the OFF-source spectra, multiplied by the system temperature and divided by the telescope gain in K Jy^{-1} units. The (ON–OFF)/OFF spectra were used to measure the rms (rms_{calib}) from a frequency range that was not affected by absorption at the reference position. (2) The individual records and polarizations of the ON-source observations were averaged, a baseline fit (2–4 order polynomial function) was subtracted, and we measured the rms (rms_{on}). (3) Averaged and baseline subtracted ON-source spectra were multiplied by $(\sqrt{2}\ rms_{on}/rms_{calib})^{-1}$ to calibrate in flux density units. To check the procedure, we reduced the IRAS 18566+0408 observations following this recipe; the resulting integrated flux density of the H_2CO absorption is consistent within 3% with the integrated flux density measured from the calibrated (ON–OFF)/OFF spectrum.

2.2. High-mass Star-forming Regions

To contrast the results from the non-HMSFR sample and verify the detection rate of H_2CO masers in high-mass star-forming regions obtained in previous surveys, we observed a sample of 22 high-mass Hi-GAL (*Herschel* infrared Galactic Plane Survey; Molinari et al. 2010) sources. Given that 6 cm H_2CO masers are typically found toward regions where other

[11] http://www.exelisvis.com/ProductsServices/IDL.aspx

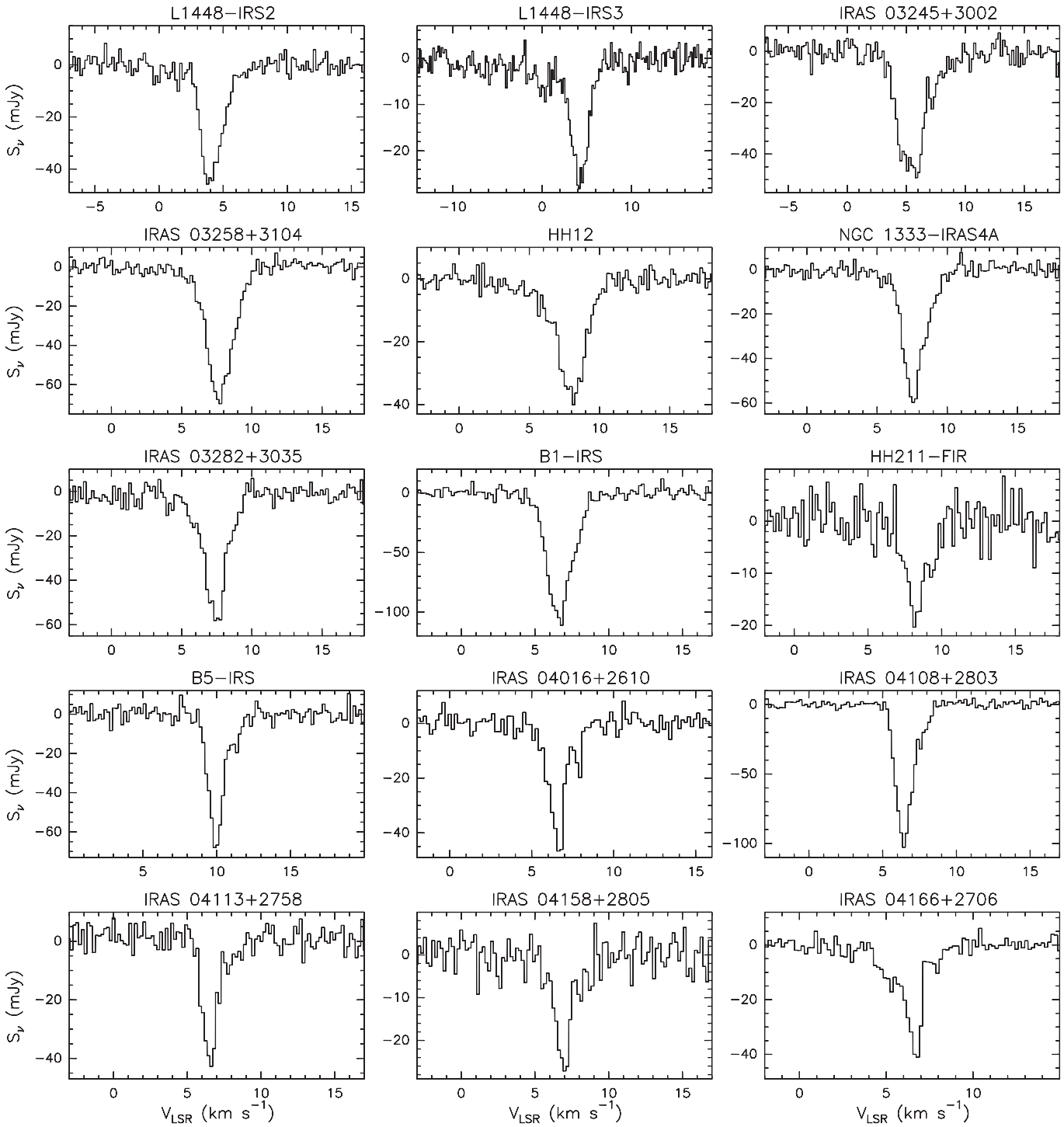

Figure 1. Spectra of 6 cm H_2CO absorption lines detected toward low-mass star-forming regions. The red asymmetry observed in some of the sources (e.g., IRAS 04016+2610, IRAS 04108+2803) is due to the $F = 1$–0 hyperfine component (Table 7).

molecular masers have previously been found (e.g., Araya et al. 2008), our selection criteria consisted of Hi-GAL sources in the Arecibo sky with 6.7 GHz CH_3OH maser detections from Olmi et al. (2014). These sources are characterized by massive ($\sim 10^2$–$10^4\ M_\odot$) and luminous ($\sim 50\ L_\odot$–$4 \times 10^3\ L_\odot$) molecular clumps in early phases of high-mass star formation. Only five of the regions in the sample may be associated with ultra-compact (UC) H II regions based on the CORNISH catalog (Hoare et al. 2012; Purcell et al. 2013). Ten of the sources have strong (>0.5 Jy) 6.7 GHz CH_3OH masers while 12 have weak (<0.5 Jy) 6.7 GHz CH_3OH masers. Six of the high-mass star-forming regions were also detected in the 6.035 GHz OH transition by Olmi et al. (2014); the other 16 were non-detections at an rms level of ∼10 mJy. Table 6 lists the high-mass star-forming regions observed in this work and the peak flux densities of 6.7 GHz CH_3OH and 6.035 GHz OH masers (see Olmi et al. 2014 for a characterization of this sample).

The observations were conducted with the Arecibo Telescope on 2014 April 9, 10, and May 7 using the C-Band receiver and WAPP spectrometer. We used a bandwidth of

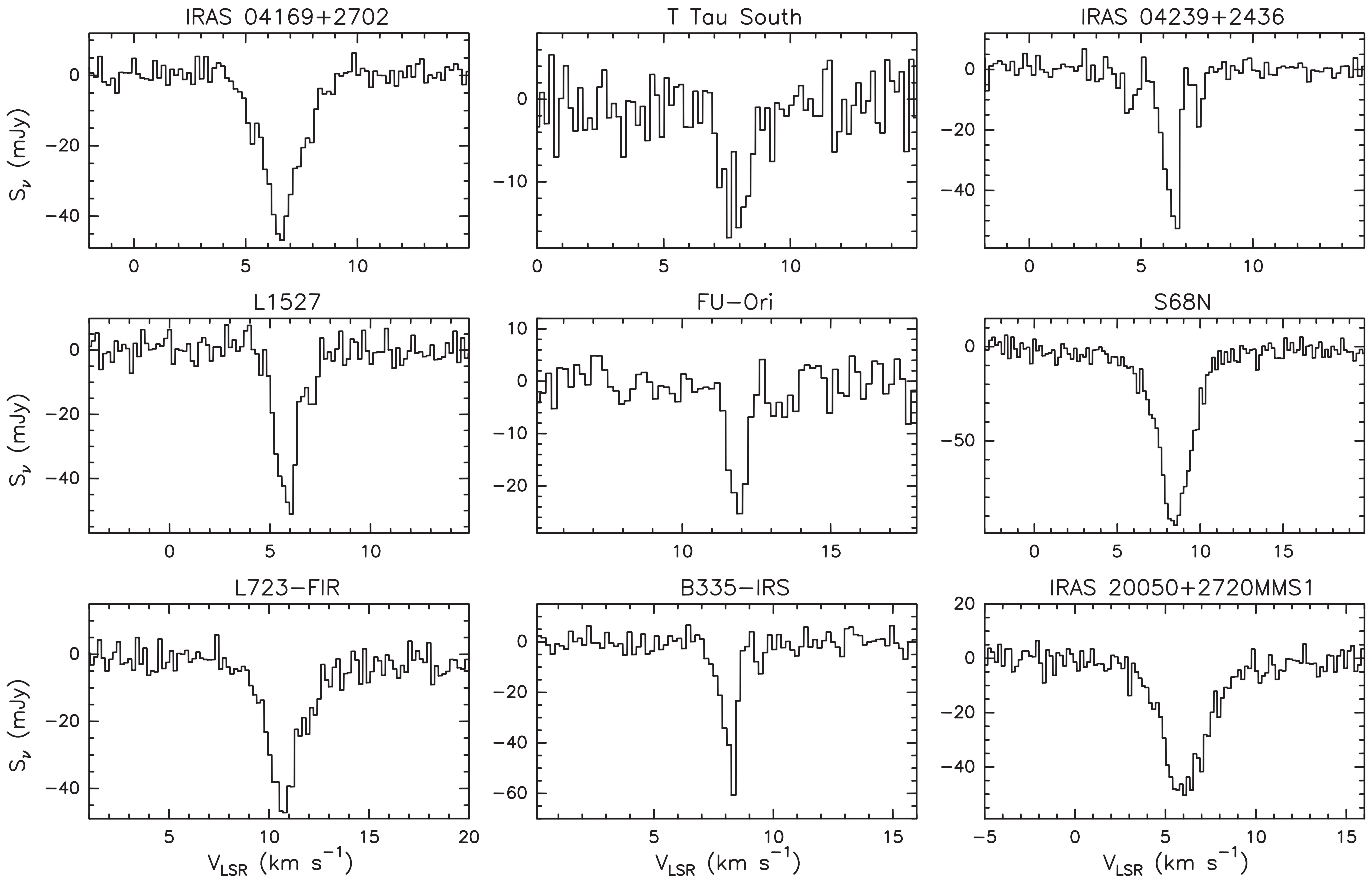

Figure 1. (Continued.)

6.25 MHz (∼400 km s^{-1}), 2048 channels (0.19 km s^{-1} channel width), centered at the 6 cm H_2CO rest frequency (4829.6594 MHz). The observations were conducted in position switching mode, with integration times of 5 minute ON and 5 minute OFF-source. We observed the Arecibo calibrator B1857+129 for system and pointing checking. Pointing errors were smaller than 7″, the system temperature was approximately 30 K and the HPBW of the telescope was approximately 0.′95. Calibration and data reduction was done in IDL using routines provided by the observatory. The calibrated spectra were exported to CLASS[12] for plotting and to measure line parameters (see Figures 2, 3, and Table 8).

3. RESULTS

We found no H_2CO emission in our sample of non HMSFRs. The typical H_2CO detection limit is $4\sigma \sim 15$ mJy (∼35 mJy in the case of the carbon stars, which were observed only 1 minute ON-source). We detected H_2CO absorption toward all but one of the observed low-mass star-forming regions; the line parameters are given in Table 7. The non-detection was toward IRAS Z04489+3032, which based on its protostellar type (Class II, Andrews & Williams 2005) appears to be a more evolved object compared to most of the other sources in the sample. Hence, IRAS Z04489+3032 is expected to have a thinner molecular envelope which could explain the H_2CO non-detection. We note that T Tau South (the other Class II source in our sample) has the weakest H_2CO absorption flux density of the detected low-mass star-forming regions, which is also consistent with thinner molecular envelopes in more evolved regions.

Figure 1 shows the spectra of all H_2CO absorption lines toward our sample of low-mass star-forming regions. Based on NVSS data (1.4 GHz, ∼0.45 mJy b^{-1} rms, $\theta_{syn} \sim 45''$, Condon et al. 1998), the H_2CO absorption appears to be against the cosmic microwave background with the possible exceptions of IRAS 04169+2702 and T Tau South. No H_2CO absorption was detected toward the sample of late-type stars at a typical rms noise of ∼4 mJy (∼9 mJy for carbon stars). We detected 6 cm H_2CO absorption toward all high-mass star-forming regions in our sample (Table 8). We also detected 6 cm H_2CO emission toward the high-mass star-forming region G32.74−0.07 (Figure 3). Based on the narrow linewidth, relatively high flux density, velocity difference with respect to systemic (as traced by H_2CO absorption), and our previous experience (Araya et al. 2004, 2005), this emission is a new 6 cm H_2CO maser.[13]

We detected an OH line at 4765.562 MHz toward the post-AGB/PPN object IRAS 04395+3601 (also known as CRL 618, V353 Aur, Westbrook Nebula). The line parameters are: S_ν =165.8 (3.7) mJy, $V_{LSR} = -59.84$ (0.01) km s^{-1}, FWHM =0.56 (0.01) km s^{-1}, where 1σ statistical errors from

[12] CLASS is part of the GILDAS software package developed by IRAM; http://www.iram.fr/IRAMFR/GILDAS.

[13] Preliminary reduction of recent VLA observations (VLA project 15A-114) has confirmed the maser nature of the emission.

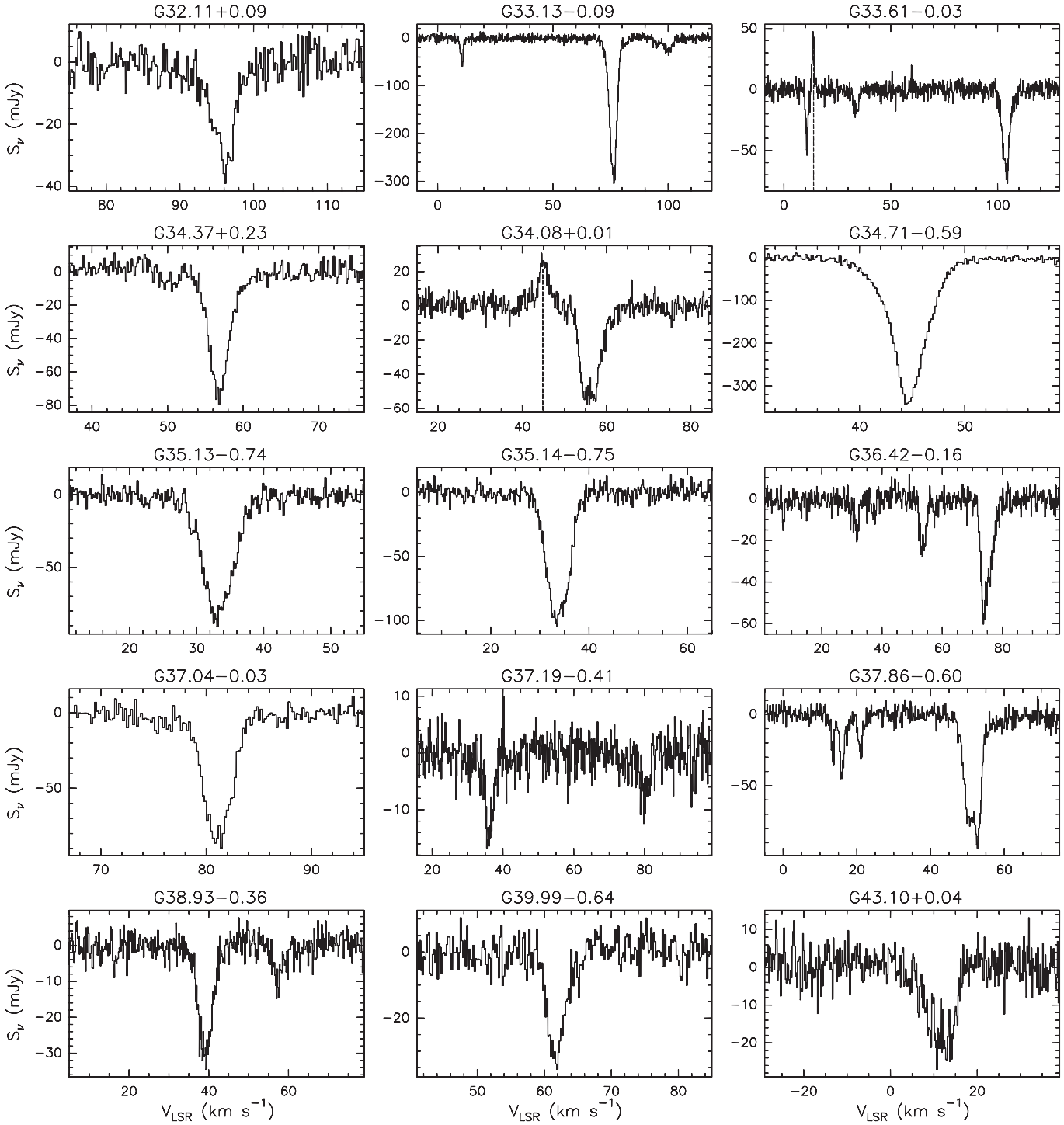

Figure 2. Spectra of 6 cm H_2CO absorption lines detected toward the sample of high-mass star-forming regions. The vertical dashed lines show absorption detected in the reference (OFF) position.

the fit are given in parenthesis. Further discussion of this detection including follow-up observations are the topic of a forthcoming paper. With the exception of IRAS 04395+3601, we detected no other spectral features of OH (4660, 4750, 4765 MHz), H110α (4874 MHz), HCOOH (4916 MHz), CH_3OH (5005 MHz), and CH_2NH (5289 MHz) toward our sample of non HMSFRs. The (4σ) detection limit for all transitions is $\sim$15 mJy ($\sim$35 mJy for carbon stars); the CH_2NH band was significantly affected by strong radio interference in all scans. The 4660 MHz OH band was also affected by interference.

4. DISCUSSION

Our previous Arecibo and VLA surveys for H_2CO masers (Araya et al. 2004, 2006a, 2008) resulted in the detection of four new H_2CO maser regions from a sample of 39 sources. Each survey consisted of 10–15 sources, and at least one new

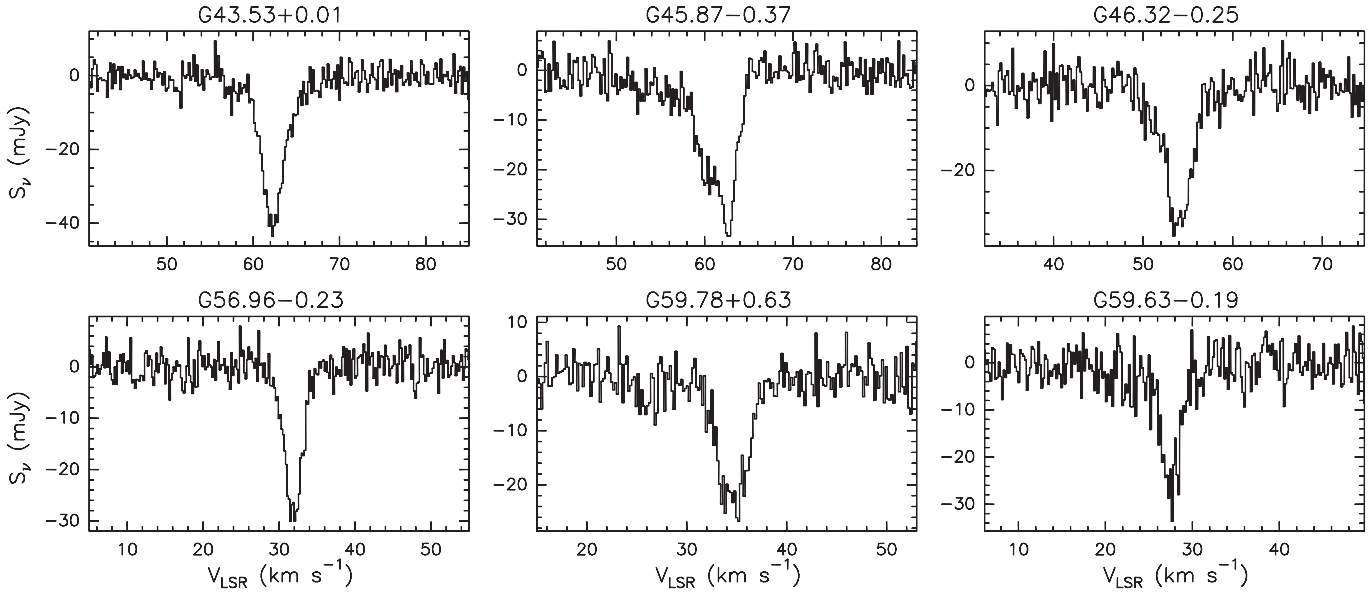

Figure 2. (Continued.)

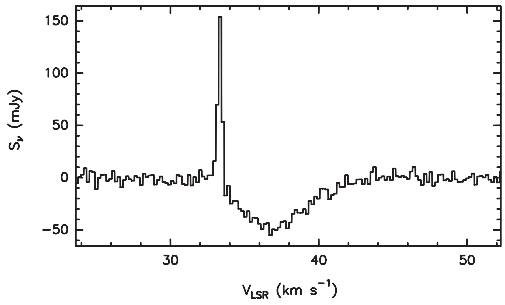

Figure 3. Detection of a new 6 cm H_2CO maser in the high-mass star-forming region G32.74−0.07 superimposed with an absorption feature.

maser region was found in every survey, i.e., a detection rate of ∼10%. The strategy to conduct these surveys was tailored to maximize the likelihood of 6 cm H_2CO maser detection by minimizing contamination from H_2CO absorption (i.e., by selecting sources with low continuum emission and by conducting interferometric observations) and/or by selecting sources rich in other molecular maser transitions, in particular Class II 6.7 GHz CH_3OH masers. Surveys for 6 cm H_2CO masers have shown that the lines are rare and weak (<2 Jy, typically ∼100 mJy; Araya et al. 2007a). In surveys for 6 cm H_2CO absorption toward IR selected high-mass star-forming regions, the detection rate of H_2CO masers is very low (non-detections in most cases), particularly when using single-dish telescopes smaller than the Arecibo Telescope (e.g., Sewiło et al. 2004; Araya et al. 2007b; Du et al. 2011; Okoh et al. 2014). Our previous surveys have shown that the low detection rate is in part a consequence of broad H_2CO absorption features masking weak H_2CO masers due to the small difference between the systemic velocity of the regions and the velocity of 6 cm H_2CO masers (Araya et al. 2007a), and the ubiquitous nature of 6 cm H_2CO absorption in high-mass star-forming regions (e.g., Watson et al. 2003).

To further check the detection rate of 6 cm H_2CO masers toward carefully selected samples of young high-mass star-forming regions, we conducted observations of the Hi-GAL sources listed in Table 6. Out of 22 sources, we detected one new 6 cm H_2CO maser (G32.74−0.07; see Table 8 and Figure 3), i.e., ∼5% detection rate. G32.74−0.07 is the eighth region in the Galaxy where 6 cm H_2CO masers have been reported (see Araya et al. 2007a, especially their Table 1, for a review of 6 cm H_2CO masers in the Galaxy). A detailed discussion of the G32.74−0.07 maser region, including VLA observations that confirm of the maser nature of the emission, is the topic of a follow-up work. If there had been the need to further optimize the survey for the detection of new 6 cm H_2CO masers (e.g., if not enough telescope time had been allocated to observe all 22 sources), we would have observed only the sub-sample of Hi-GAL sources with bright (>0.5 Jy) 6.7 GHz CH_3OH masers and with evidence for rich maser activity from other molecular species, i.e., with detections of 6.035 GHz OH masers. Only five sources from Table 6 have these characteristics; one of them is the new 6 cm H_2CO maser region, which would imply a detection rate of ∼20% in a sample of young high-mass star-forming regions with evidence for rich maser activity. Therefore, despite the small number of sources, the observations of this new set of high-mass star-forming regions are consistent with a ∼10% detection rate of 6 cm H_2CO masers in carefully selected samples.[14]

The combined samples of evolved stellar objects (late-type stars, PPN and PN) and low-mass star-forming regions observed in this work have more than 20 sources each, thus, similar to the number of sources observed in each one of our previous Arecibo and VLA surveys (including the observations of the Hi-GAL sample from this work). By nature, our sample of non HMSFRs is significantly less affected by H_2CO absorption that can potentially mask emission. The rms noise in this work (∼4 mJy) is similar to, or better than, the sensitivity limits of previous surveys. Thus, the non-detection of H_2CO masers toward non HMSFRs supports the hypothesis

[14] We stress that, as in previous dedicated surveys for 6 cm H_2CO masers (see Araya et al. 2007a), small samples imply few detections, and therefore, detection rate values must be considered as rough estimates.

Table 7
H_2CO Line Parameters: Low-mass Star-forming Regions

Source	rms (mJy)	S_ν (mJy)	V_{LSR} (km s^{-1})	FWHM (km s^{-1})	$\int S_\nu dv$ (mJy km s^{-1})	Notes
L1448-IRS2	2.7	−45.8	3.8 (0.2)	2.1 (0.4)	−88 (2)	1
L1448-IRS3	2.3	−28.2	4.2 (0.2)	2.3 (0.4)	−67 (2)	1
IRAS 03245+3002	3.4	−49.2	5.9 (0.2)	2.5 (0.4)	−137 (3)	⋯
IRAS 03258+3104	2.6	−69.7	7.8 (0.2)	2.1 (0.4)	−151 (2)	1
HH12	2.2	−40.1	8.1 (0.2)	1.9 (0.4)	−99 (2)	1
NGC 1333-IRAS4A	2.4	−59.7	7.6 (0.2)	1.9 (0.4)	−110 (2)	1
IRAS 03282+3035	3.2	−58.1	7.4 (0.2)	1.3 (0.4)	−125 (3)	⋯
B1-IRS	4.0	−111.0	6.8 (0.2)	1.9 (0.4)	−219 (4)	⋯
HH211-FIR	3.3	−20.3	8.1 (0.2)	1.1 (0.4)	−33 (3)	⋯
B5-IRS	3.3	−68.0	9.9 (0.2)	1.1 (0.4)	−92 (2)	⋯
IRAS 04016+2610	3.0	−46.6	6.6 (0.2)	0.8 (0.4)	−62 (2)	⋯
IRAS 04108+2803	2.2	−102.7	6.4 (0.2)	1.3 (0.4)	−147 (2)	1
IRAS 04113+2758	3.5	−42.7	6.6 (0.2)	1.1 (0.4)	−56 (3)	⋯
IRAS 04158+2805	3.7	−27.1	7.0 (0.2)	1.1 (0.4)	−42 (3)	⋯
IRAS 04166+2706	2.1	−41.0	6.8 (0.2)	1.0 (0.4)	−64 (2)	1
IRAS 04169+2702	2.2	−46.8	6.6 (0.2)	1.7 (0.4)	−91 (2)	1
T Tau South	3.7	−16.8	7.6 (0.2)	1.3 (0.4)	−17 (2)	⋯
IRAS 04239+2436	2.5	−52.6	6.6 (0.2)	0.8 (0.4)	−43 (1)	1
	⋯	−18.9	⋯	<0.4	−7 (1)	2, 3
	⋯	−14.4	4.4 (0.2)	0.6 (0.4)	−8 (1)	⋯
L1527	3.1	−51.0	6.1 (0.2)	1.3 (0.4)	−62 (4)	⋯
IRAS Z04489+3032	3.7	<15	⋯	⋯	⋯	⋯
FU-Ori	3.3	−25.3	11.9 (0.2)	0.8 (0.4)	−19 (2)	⋯
S68N	4.0	−94.8	8.5 (0.2)	2.1 (0.4)	−250 (4)	⋯
L723-FIR	3.4	−47.2	10.8 (0.2)	1.3 (0.4)	−108 (4)	⋯
B335-IRS	3.3	−60.7	8.3 (0.2)	0.6 (0.4)	−41 (2)	⋯
	⋯	−12.6	⋯	<0.4	−5 (1)	2, 3
IRAS 20050+2720MMS1	3.5	−50.4	6.1 (0.2)	2.7 (0.4)	−151 (4)	⋯

Note. We list the intensity of the peak channel, the LSR velocity of the peak channel (channel separation reported as uncertainty) and FWHM (two times the channel separation is reported as uncertainty). The $\int S_\nu dv$ uncertainty is rms × channel separation × square root of the number of channels in the line. (1) H_2CO absorption detected in the reference (OFF) position. (2) The $F = 1-0$ hyperfine transition is *not* blended with the main absorption line, thus we also list the line parameters of the $F = 1-0$ component. (3) The line was only detected in two channels at the half maximum flux density level.

that H_2CO masers are less common (and/or less intense) in late-type stars and low-mass star-forming region environments in comparison to high-mass star-forming regions. Indeed, at present, H_2CO masers have *only* been detected toward regions of high-mass star formation.

It is worth noting that among the known masers, several species such as OH and H_2O are detected in a variety of astrophysical environments (e.g., low and high-mass star-forming regions, late-type stars), whereas other maser species appear to be tracers of specific environments, e.g., Class II methanol masers have been detected only toward regions of high-mass star formation (Minier et al. 2003; Pandian et al. 2011; Breen et al. 2013; Urquhart et al. 2015).[15] Although the number of non HMSFRs observed in this work is small, the observations presented here, together with other H_2CO surveys reported in the literature, support the idea that the conditions required to excite 6 cm H_2CO masers to detectable levels ($\gtrsim$30 mJy) are exclusively found in high-mass star-forming regions. Specifically, the known 6 cm H_2CO masers are located in regions where active high-mass star formation is evident based on the detection of nearby UC H II regions, high infrared luminosities, hot molecular cores and/or other maser species. However, with the exception of some 6 cm H_2CO maser regions in Sgr B2 (e.g., Mehringer et al. 1994), most 6 cm H_2CO masers do not seem to be *directly* associated with UC H II regions, but instead, they are associated with younger phases of high-mass star formation characterized by hot molecular core environments, hyper-compact H II regions and/or weak (or undetectable) radio continuum sources (e.g., Araya et al. 2007a, 2007c, 2008). Even though a fully satisfactory theoretical explanation for H_2CO masers has not been achieved yet, the current H_2CO maser pumping models require special physical conditions in terms of density, abundance, coherent path length, and/or high emission measure from a background H II region (Boland & de Jong 1981; van der Walt 2014), thus the exclusive association of H_2CO masers with high-mass star-forming regions is also expected from a theoretical perspective.

5. SUMMARY

We report the first survey specifically intended to search for H_2CO maser emission toward non HMSFRs. A total of 71 non HMSFRs were observed, 25 low-mass star-forming regions, 31 late-type stars, and 15 post-AGB to PN objects. No maser was detected down to a sensitivity limit of 15 mJy (~4σ; 35 mJy in a subsample of eight carbon stars). We also conducted observations of a sample of 22 young high-mass star-forming regions from the Hi-GAL sample of Olmi et al. (2014) to compare to the results from the non-HMSFR sample. We

[15] Note however that Class I methanol masers have been detected toward high-mass and low-mass star-forming regions, and near supernova remnants; e.g., Kurtz et al. (2004), Kalenskii et al. (2013), McEwen et al. (2014).

Table 8
H_2CO Line Parameters: Hi-GAL Sample

Source	rms (mJy)	S_ν (mJy)	V_{LSR} (km s^{-1})	FWHM (km s^{-1})	$\int S_\nu dv$ (mJy km s^{-1})	Notes
G32.11+0.09	4.6	−31.1	95.9 (0.1)	3.8 (0.3)	−126 (6)	⋯
G32.74−0.07	4.6	−12.1	10.0 (0.1)	1.4 (0.3)	−18 (3)	⋯
	⋯	164.0	33.33 (0.01)	0.36 (0.01)	62 (2)	⋯
	⋯	−48.3	37.00 (0.07)	5.0 (0.2)	−259 (8)	⋯
G33.13−0.09	5.2	−55.4	10.50 (0.03)	1.33 (0.09)	−78 (4)	⋯
	⋯	−292.3	76.17 (0.02)	3.72 (0.05)	−1158 (12)	⋯
	⋯	−12.8	95.2 (0.2)	2.7 (0.5)	−36 (7)	⋯
	⋯	−28.1	100.1 (0.1)	4.2 (0.4)	−124 (9)	⋯
G33.61−0.03	4.6	−50.2	10.75 (0.08)	1.1 (0.2)	−60 (9)	1
	⋯	−18.7	33.7 (0.4)	2.8 (0.8)	−56 (14)	⋯
	⋯	−67.5	103.94 (0.04)	4.0 (0.1)	−289 (6)	⋯
G34.37+0.23	4.4	−72.0	56.83 (0.04)	3.16 (0.09)	−242 (6)	2
G34.08+0.01	4.9	−56.5	56.21 (0.06)	5.3 (0.1)	−321 (7)	3
G34.71−0.59	5.0	−167.9	44.64 (0.02)	5.5 (0.1)	−990 (34)	4
	5.0	−168.6	44.75 (0.01)	2.48 (0.09)	−446 (38)	4
G35.13−0.74	4.6	−82.8	33.20 (0.04)	5.4 (0.1)	−478 (7)	⋯
G35.14−0.75	4.9	−102.0	33.70 (0.03)	5.26 (0.08)	−571 (7)	⋯
G36.42−0.16	4.0	−14.7	7.2 (0.2)	0.7 (0.4)	−10 (6)	⋯
	⋯	−14.1	31.4 (0.4)	2 (1)	−34 (15)	⋯
	⋯	−25.8	53.6 (0.2)	2.3 (0.4)	−63 (11)	⋯
	⋯	−34.3	73.53 (0.05)	1.6 (0.3)	−59 (17)	5
	⋯	−37.8	75.3 (0.2)	4.0 (0.3)	−161 (20)	5
G37.04−0.03	4.5	−85.5	81.09 (0.03)	3.14 (0.07)	−286 (6)	⋯
G37.19−0.41	3.0	−14.6	36.2 (0.1)	2.8 (0.3)	−44 (3)	⋯
G37.86−0.60	4.8	−31.8	13.53 (0.05)	0.8 (0.1)	−28 (3)	⋯
	⋯	−40.2	15.99 (0.05)	1.6 (0.2)	−68 (5)	⋯
	⋯	−26.7	20.96 (0.07)	1.4 (0.2)	−40 (4)	⋯
	⋯	−71.4	50.3 (0.1)	3.2 (0.3)	−242 (23)	5
	⋯	−74.3	52.96 (0.09)	2.3 (0.2)	−184 (22)	5
G38.93−0.36	3.0	−30.9	39.14 (0.06)	4.1 (0.1)	−135 (4)	⋯
	⋯	−9.5	57.4 (0.2)	3.2 (0.4)	−32 (3)	⋯
G39.99−0.64	4.4	−32.3	61.77 (0.07)	3.0 (0.2)	−103 (5)	⋯
G43.10+0.04	4.6	−20.8	11.8 (0.1)	6.9 (0.3)	−152 (6)	⋯
G43.53+0.01	2.7	−38.9	62.34 (0.05)	3.4 (0.1)	−139 (4)	⋯
G45.87−0.37	2.9	−21.0	60.7 (0.2)	4.8 (0.4)	−107 (10)	5
	⋯	−19.5	62.84 (0.07)	1.7 (0.2)	−35 (7)	5
G46.32−0.25	4.0	−32.4	53.92 (0.07)	3.6 (0.2)	−124 (5)	⋯
G56.96−0.23	2.6	−29.1	31.89 (0.04)	2.8 (0.1)	−86 (3)	⋯
G59.78+0.63	3.3	−24.1	34.61 (0.08)	3.5 (0.2)	−89 (4)	⋯
G59.63−0.19	3.8	−26.1	27.51 (0.08)	2.7 (0.2)	−75 (5)	⋯

Note. Line parameters from Gaussian fits, 1σ statistical errors from the fit are listed in parenthesis. (1) Absorption detected in reference position (13.7 km s^{-1}). (2) Absorption detected in reference position (35.8 km s^{-1}). (3) Absorption detected in reference position (45.0 km s^{-1}). (4) Asymmetric spectral line with broad spectral line wings fitted with two Gaussians. (5) Two Gaussian profiles used to fit overlapping spectral lines.

detected a 6 cm H_2CO maser in the high-mass star-forming region G32.74−0.07. Therefore, our work supports the hypothesis that H_2CO masers are a phenomenon exclusively associated with the process of high-mass star formation.

We detected no H_2CO absorption toward late-type stars, but detected absorption toward all but one of the low-mass star-forming regions. The absorption appears to be against the cosmic microwave background in most cases. We detected 6 cm H_2CO absorption toward all the sources in our sample of high-mass star-forming regions.

For the non HMSFRs, we conducted a simultaneous survey for OH (4660, 4750, 4765 MHz), H110α (4874 MHz), HCOOH (4916 MHz), CH_3OH (5005 MHz), and CH_2NH (5289 MHz) toward 68 of the 71 sources. The CH_2NH observations were severely affected by radio interference, thus detection limits cannot be reliably given. With the exception of the post-AGB object IRAS 04395+3601 for which we detected 4765 MHz OH emission, we did not detect any other emission/absorption line down to a sensitivity limit of 15 mJy (4σ; 35 mJy for carbon stars).

We thank the anonymous referee for critically reading the manuscript and for valuable suggestions. This work has made use of the computational facilities donated by Frank Rodeffer to the Astrophysics Research Laboratory of Western Illinois University. This work was partially motivated by conversations with E. Churchwell and from input of the anonymous referee of Araya et al. (2007c). P.H. and M.C.E. acknowledge partial support from NSF grant AST-0908901. S.K. acknowledges partial support from UNAM, DGAPA project IN 114514. This research made

use of the NASA's Astrophysics Data System, the VizieR catalog access tool (CDS, Strasbourg, France), and SIMBAD.

REFERENCES

Alksnis, A., Balklavs, A., Dzervitis, U., et al. 2001, BaltA, 10, 1
Andrews, S. M., & Williams, J. P. 2005, ApJ, 631, 1134
Araya, E., Hofner, P., Goldsmith, P., Slysh, S., & Takano, S. 2003, ApJ, 596, 556
Araya, E., Hofner, P., & Goss, W. M. 2007a, in IAU Symp. 242, Astrophysical Masers and their Environments, ed. J. M. Chapman & W. A. Baan (Cambridge: Cambridge Univ. Press), 110
Araya, E., Hofner, P., Goss, W. M., et al. 2006a, ApJL, 643, L33
Araya, E., Hofner, P., Goss, W. M., et al. 2007b, ApJS, 170, 152
Araya, E., Hofner, P., Kurtz, S., et al. 2005, ApJ, 618, 339
Araya, E., Hofner, P., Linz, H., et al. 2004, ApJS, 154, 579
Araya, E., Hofner, P., Olmi, L., Kurtz, S., & Linz, H. 2006b, AJ, 132, 1851
Araya, E., Hofner, P., Sewiło, M., et al. 2007c, ApJ, 669, 1050
Araya, E. D., Dieter-Conklin, N., Goss, W. M., & Andreev, N. 2014, ApJ, 784, 129
Araya, E. D., Hofner, P., Goss, W. M., et al. 2008, ApJS, 178, 330
Benson, P. J., Little-Marenin, I. R., Woods, T. C., et al. 1990, ApJS, 74, 911
Boland, W., & de Jong, T. 1981, A&A, 98, 149
Bontemps, S., Andre, P., Terebey, S., & Cabrit, S. 1996, A&A, 311, 858
Breen, S. L., Ellingsen, S. P., Contreras, Y., et al. 2013, MNRAS, 435, 524
Colgan, S. W. J., Salpeter, E. E., & Terzian, Y. 1986, AJ, 91, 107
Condon, J. J., Cotton, W. D., Greisen, E. W., et al. 1998, AJ, 115, 1693
Dieter, N. H. 1973, ApJ, 183, 449
Downes, D., & Wilson, T. L. 1974, ApJL, 191, L77
Downes, D., Wilson, T. L., Bieging, J., & Wink, J. 1980, A&AS, 40, 379
Du, Z. M., Zhou, J. J., Esimbek, J., Han, X. H., & Zhang, C. P. 2011, A&A, 532, A127
Few, R. W. 1979, MNRAS, 187, 161
Forster, J. R., Goss, W. M., Gardner, F. F., & Stewart, R. T. 1985, MNRAS, 216, 35
Forster, J. R., Goss, W. M., Wilson, T. L., Downes, D., & Dickel, H. R. 1980, A&A, 84, L1
Furuya, R. S., Kitamura, Y., Wootten, A., Claussen, M. J., & Kawabe, R. 2003, ApJS, 144, 71
Garrison, B. J., Lester, W. A., Miller, W. H., & Green, S. 1975, ApJL, 200, L175
Gordon, M. A., & Sorochenko, R. L. 2002, Radio Recombination Lines: Their Physics and Astronomical Applications (1st ed.; Dordrecht: Kluwer)
Goss, W. M., Manchester, R. N., Brooks, J. W., et al. 1980, MNRAS, 191, 533
Gramajo, L. V., Rodón, J. A., & Gómez, M. 2014, AJ, 147, 140
Green, J. D., Evans, N. J., II, Kóspál, Á, et al. 2013, ApJ, 772, 117
Harvey-Smith, L., & Cohen, R. J. 2005, MNRAS, 356, 637
Heiles, C. 1973, ApJ, 183, 441
Hoare, M. G., Purcell, C. R., Churchwell, E. B., et al. 2012, PASP, 124, 939
Hoffman, I. M., Goss, W. M., Palmer, P., & Richards, A. M. S. 2003, ApJ, 598, 1061
Kalenskii, S. V., Kurtz, S., & Bergman, P. 2013, ARep, 57, 120
Kalenskii, S. V., Slysh, V. I., Goldsmith, P. F., & Johansson, L. E. B. 2004, ApJ, 610, 329
Kohoutek, L. 2001, A&A, 378, 843
Kurtz, S., Hofner, P., & Álvarez, C. V. 2004, ApJS, 155, 149
Marscher, A. P., Moore, E. M., & Bania, T. M. 1993, ApJL, 419, L101
Martin, R. N., & Barrett, A. H. 1978, ApJS, 36, 1
McEwen, B. C., Pihlström, Y. M., & Sjouwerman, L. O. 2014, ApJ, 793, 133
Mehringer, D. M., Goss, W. M., & Palmer, P. 1994, ApJ, 434, 237
Mehringer, D. M., Goss, W. M., & Palmer, P. 1995, ApJ, 452, 304
Minier, V., Ellingsen, S. P., Norris, R. P., & Booth, R. S. 2003, A&A, 403, 1095
Minn, Y. K., & Greenberg, J. M. 1973, A&A, 22, 13
Molinari, S., Swinyard, B., Bally, J., et al. 2010, PASP, 122, 314
Moore, E. M., & Marscher, A. P. 1995, ApJ, 452, 671
Müller, H. S. P., Menten, K. M., & Mäder, H. 2004, A&A, 428, 1019
Okoh, D., Esimbek, J., Zhou, J. J., et al. 2014, Ap&SS, 350, 657
Olmi, L., Araya, E. D., Hofner, P., et al. 2014, A&A, 566, A18
Palmer, P., Zuckerman, B., Buhl, D., & Snyder, L. E. 1969, ApJL, 156, L147
Pandian, J. D., Momjian, E., Xu, Y., Menten, K. M., & Goldsmith, P. F. 2011, ApJ, 730, 55
Pettersson, B. 1987, A&A, 171, 101
Pickett, H. M., Poynter, R. L., Cohen, E. A., et al. 1998, JQSRT, 60, 883
Pratap, P., Menten, K. M., & Snyder, L. E. 1994, ApJL, 430, L129
Purcell, C. R., Hoare, M. G., Cotton, W. D., et al. 2013, ApJS, 205, 1
Quanz, S. P., Henning, T., Bouwman, J., et al. 2007, ApJ, 668, 359
Rodríguez, M. I., Allen, R. J., Loinard, L., & Wiklind, T. 2006, ApJ, 652, 1230
Rots, A. H., Dickel, H. R., Forster, J. R., & Goss, W. M. 1981, ApJL, 245, L15
Sandqvist, A., & Bernes, C. 1980, A&A, 89, 187
Sandqvist, A., & Lindroos, K. P. 1976, A&A, 53, 179
Sewiło, M., Watson, C., Araya, E., et al. 2004, ApJS, 154, 553
Snyder, L. E., Buhl, D., Zuckerman, B., & Palmer, P. 1969, PhRvL, 22, 679
Townes, C. H., & Cheung, A. C. 1969, ApJL, 157, L103
Tucker, K. D., Tomasevich, G. R., & Thaddeus, P. 1970, ApJL, 161, L153
Turner, B. E. 1994, ApJ, 437, 658
Urquhart, J. S., Moore, T. J. T., Menten, K. M., et al. 2015, MNRAS, 446, 3461
van der Walt, D. J. 2014, A&A, 562, A68
Vanden Bout, P. A., Snell, R. L., & Wilson, T. L. 1983, A&A, 118, 337
Watson, C., Araya, E., Sewilo, M., et al. 2003, ApJ, 587, 714
Whiteoak, J. B., & Gardner, F. F. 1974, A&A, 37, 389
Whiteoak, J. B., & Gardner, F. F. 1983, MNRAS, 205, 27
Young, K. E., Lee, J.-E., Evans, N. J., II, Goldsmith, P. F., & Doty, S. D. 2004, ApJ, 614, 252
Zacharias, N., Urban, S. E., Zacharias, M. I., et al. 2003, yCat, 1289, 0
Zhou, S., Evans, N. J., II, Butner, H. M., et al. 1990, ApJ, 363, 168